- Optimization of batch and packed-bed column Cr (VI) adsorption
- of an amine-rich chitosan/polyethyleneimine composite: Application
- in electroplating wastewater treatment

Ali Ansari a^{ϕ} , Raynara Maria Silva Jacovone a^{ϕ} , Enrico Tapire Nadres a^{α} , Minh $D\tilde{o}^{\alpha}$, Debora Frigi Rodrigues a* ^a Department of Civil and Environmental Engineering, Room N136 Engineering Building 1, University of Houston, TX 77204-4003 (U.S.A.) ϕ Equal contribution *Corresponding Author: Email: dfrigirodrigues@uh.edu; Phone: +1-713-743-1495

Abstract

Toxic oxyanions of Cr (VI) can be potentially removed by adsorbents with positively charged surfaces. In this study, we synthesized a stable and insoluble amine-rich polymer composite (CS-PEI-GLA) by crosslinking polyethyleneimine (PEI), a soluble amine-rich synthetic polymer, and chitosan (CS) with glutaraldehyde (GLA). The positively charged amine groups were the main adsorption sites. The batch investigation demonstrated that the adsorbent was able to remove ≥90% of chromium in pH ranging from 2 to 8. Due to deprotonation of the amine groups, chromium removal decreased at higher pH values. The adsorption was fast and reached equilibrium after 45 min. The maximum adsorption capacity was 500 mg/g according to the Langmuir isotherm and did not decrease in the presence of monovalent anions. In the column study, the adsorption capacity was the highest when the flow rate was the lowest (5 mL/min), influent concentration was medium (225 mg/L), and the bed height was the shortest (3.5 cm). NaOH was the best recovery reagent with recovery of 67% in batch and 31% in the column. The CS-PEI-GLA was able to remove 97.1 ± 0.1% chromium in batch and treat 750 mL of electroplating wastewater with a 3.5 cm packed-bed column.

Keywords: Chitosan, Polyethyleneimine, Chromium, Batch adsorption, Packed-bed column

1. Introduction

40

41

42

43

44

45

46

47

48

49

50

51

52

53

54

55

56

57

58

59

60

61

62

Chromium is mainly present in the environment as Cr (III) and Cr (VI) (1-5). Cr (III) is a micronutrient, but it can be toxic at high concentrations. On the other hand, Cr (VI) compounds like chromate (CrO₄⁻), dichromate (Cr₂O₇²-), and hydrogen chromate (HCrO₄) are carcinogenic and toxic even at ppb levels since they are highly soluble and can easily diffuse through the cell membranes in the tissues (1, 6-8). These harmful compounds are usually found in electroplating wastewater, leather tanning, nuclear power, metal finishing, photography, dying, and textile industries (1, 6, 7, 9). The environmental threat of Cr (VI) has attracted many scientists to work on innovative approaches to remove Cr (VI) from water for the past 20 years, as indicated by the high number of publications. (4, 5) Furthermore, many studies have favored adsorption over other methods, mainly because it is simple, cost-effective, and reusable (1, 3-5, 10). Two review articles from 2008 (11) and 2023 (12) have identified coagulation/flocculation followed by filtration as a promising industrial approach for Cr (VI) removal. This means that despite all the research done, no significant practical advances have been made for chromium treatment that has been applied in industry. The main missing piece in many of these past adsorption studies is how the adsorbent can be used in real-world applications. For instance, nano scale adsorbents are popular for chromium removal among scientists, (13, 14) however, the high surface energy of these adsorbents leads to aggregation, which makes the adsorption sites unavailable for chromium removal, making the adsorbent inefficient.(15) That could be the reason why most research articles limit the evaluation of their adsorbents to batch conditions instead of continuous conditions, like in a column reactor. To put this fact into numbers, in a review article focusing on polyethyleneimine (PEI) composites, (5) out of 136 studies on chromium adsorption, only six had studied continuous flow

conditions in a column reactor. While the authors highlight the value of batch studies as an essential first step to understand the adsorption process, they emphasized the importance of investigations in flow conditions to bring adsorption technologies to real-world applications. Moreover, to improve the reusability in industrial scale applications, large size adsorbents are more desirable (15-17). The literature review has shown that for the removal of anionic Cr (VI) compounds, an adsorbent with abundant positively charged functional groups like -NH₂ can be effective.(1, 18, 19) Chitosan (CS) and PEI are two amine-rich polymers that have been described to be good candidates for chromium removal. CS is a cheap, natural polymer that can be produced from the waste of shrimp canning industry.(20) PEI is a synthetic polymer with repeating -CH₂CH₂N- groups.(5) The two polymers are naturally unstable especially at acidic pHs, therefore they should be combined with other materials to form a stable composite. (21-41) Previous studies have identified two main problems in CS/PEI adsorbents used for metal removal: 1. Complicated synthesis process (42, 43) and 2. Reduction in adsorption capacity at pH values above 3 that would lead to low adsorption capacity at neutral pH value.(42-46) To use an adsorbent for chromium removal in industry, the production process should be robust to facilitate scale-up and the adsorbent should be effective at pH values close to real wastewater, instead of highly acidic water. This study fills these knowledge gaps and lays a foundation for real-world application of these two promising polymers for chromium adsorption. A facile synthesis method at room temperature was used to synthesize a durable composite of chitosan and polyethyleneimine using glutaraldehyde (GLA) as the crosslinker (CS-PEI-GLA). After conducting the mechanistic studies to understand the fundamentals of adsorption in batch mode, including the effect of PEI concentration, pH, dosage, contact time, initial Cr (VI) concentration, and coexisting ions on Cr (VI) adsorption. The

63

64

65

66

67

68

69

70

71

72

73

74

75

76

77

78

79

80

81

82

83

84

practicality of the adsorbent was investigated by packing a column with the adsorbent for continuous removal of Cr (VI). Effect of flow rate, concentration of chromium (VI) in the influent, and bed height on the column performance was studied. Recovery of the adsorbent in both batch and continuous modes were studied with different recovery agents at different concentrations, and finally, chromium removal from real electroplating wastewater was done by CS-PEI-GLA.

2. Materials and methods

2.1. Preparation of the CS-PEI-GLA adsorbents and characterization

The synthesis procedure of the adsorbents and the characterization techniques can be found in our previous publications.(20, 47) Briefly, different solutions with fixed concentration of chitosan (2% w/w) and four different concentrations of polyethyleneimine (0, 2, 5, 10% w/w) were prepared. The solutions were stirred overnight, and after that, glutaraldehyde was added to the ultimate chitosan concentration of 2% w/w. The solutions were transformed into gels after GLA (2%) addition. The gels were washed several times with deionized water and freeze-dried. Different techniques used to characterize the adsorbent were Attenuated Total Reflectance Fourier Transform Infrared spectroscopy (ATR-FTIR), Brunauer-Emmett-Teller (BET), X-ray photoelectron spectroscopy (XPS), and Scanning Electron Microscopy (SEM) as described by Nadres et al. (47).

2.2. Optimization of Cr (VI) removal: Batch process

The batch process was used to optimize Cr (VI) removal in terms of PEI concentration in the adsorbent, pH, dosage of the adsorbent, time of exposure of Cr (VI) to the adsorbent, and initial concentration of Cr (VI). The effect of temperature and coexisting ions on the adsorption was also investigated. The general procedure for Cr (VI) removal was as follows: CS-PEI-GLA dry powder was mixed with Cr (VI) solution and shaken at 120 rpm for the time indicated. Then, the

suspension was allowed to settle, and an aliquot was withdrawn. The solution was filtered through a sterile syringe filter with polyethersulfone (PES) membrane with 0.2 µm pore size (VWR). The chromium concentration in the samples were measured by atomic absorption spectroscopy (AAS) using PerkinElmer AAnalyst 200. Seven solutions with 1 to 7 mg/L of chromium were prepared as calibration standards. The details for each set of experiments are described in the supporting information. All experiments were done in triplicates and the percent removal was calculated with **Equation 1** and adsorption capacity at equilibrium (qeq) with **Equation 2**:

116
$$Removal(\%) = \frac{c_i - c_e}{c_i} \times 100$$
 Equation (1)

where C_i (mg/L) is the initial concentration and C_e (mg/L) is the equilibrium concentration of chromium.

119
$$q_{eq}(\frac{mg}{g}) = \frac{(C_i - C_e) \times V}{m}$$
 Equation (2)

where V (L) is the volume of sample and m (g) is the mass of the adsorbent.

2.3. Optimization of Cr (VI) removal: Column process

The details of the column setup are provided in the supporting information. The effect of flow rate was investigated with 0.5 g of the polymer composite (equal to 7 cm bed height) packed in the column. Then, 225 mg/L Cr (VI) was pumped through the column at three different rates (5, 7.5, and 10 mL/min). The flow rate was adjusted by changing the pump's speed and measured by measuring the effluent volume in 1 min. The effect of influent concentration was investigated at the best flow rate (5 mL/min) with 0.5 g (7 cm) of the adsorbent packed in the column. Cr (VI) solutions with concentrations of 100, 225, and 500 mg/L were pumped through the column. The effect of packed-bed height on Cr (VI) removal was investigated at the optimized flow rate (5

mL/min) and initial Cr (VI) concentration (225 mg/L). Three bed heights were tested by packing the glass column with 0.25 (3.5 cm), 0.5 (7 cm), and 0.75 g (10.5 cm) of CS-PEI-GLA.

2.4. Recovery of chromium from CS-PEI-GLA in batch and continuous modes

CS-PEI-GLA (0.5 g) was exposed to 200 mL of 1000 mg/L Cr (VI) for 3 h. Then, the suspension was allowed to settle. The adsorbent was collected and washed with deionized water twice. Excess water was removed by placing the precipitates on a paper towel. Recovery of chromium ions was started by weighing 20 mg of the Cr (VI)-laden CS-PEI-GLA and adding it to 40 mL of recovery reagents. The recovery reagents used were water, HCl (0.1 M), NaOH (0.1 M), Na₂SO₄ (0.1 M), NaCl (0.1 M), NaHCO₃ (0.1 M). The mixtures were shaken for 24 h and analyzed for total chromium concentration by AAS as described in section 2.2. The recovery percentage was calculated by **Equation 3**:

141
$$Cr Recovered (\%) = \frac{c_d}{c_i - c_e} \times 100$$
 Equation (3)

where C_d (mg/L) is the chromium concentration in the supernatant after desorption and C_i and C_e (mg/L) are the same as described in section 2.2. For the best recovery reagent, different concentrations (0.1, 0.25, 0.50 and 1.0 M) and three adsorption/desorption cycles were tested. The adsorbents before and after adsorption, and after desorption cycles were characterized with ATR-FTIR and XPS. The optimized recovery agent was used to recover chromium from a saturated column. First, the column with 0.5 g of the adsorbent was saturated with 225 mg/L Cr (VI) solution at 5 mL/min for 8 h. Then, 200 mL of the recovery agent was run through the column at 5 mL/min and 10 mL fraction of the eluent was collected to measure the chromium concentration.

2.5. Removal of chromium from electroplating wastewater in batch and continuous modes

A 200 mL of electroplating wastewater obtained from Allied Plating, Houston, TX was mixed with 100 mg of CS-PEI-GLA. The wastewater was used without prior pretreatment. The mixture was left in a shaker for 1 h. After that, the suspension was allowed to settle, and an aliquot was withdrawn. Chromium concentration was measured as described in section 2.2. For continuous removal of chromium from the plating wastewater, a column was prepared with 0.25 g of the adsorbent as described before. Wastewater was pumped through the column at 5 mL/min. Fractions of 25 mL were collected for 6 h and chromium concentrations were analyzed as described in section 2.2.

3. Results and discussion

3.1. Optimization of Cr (VI) removal in batch mode

3.1.1. Optimization of PEI concentration

Four adsorbents with different PEI contents, 0, 2, 5, and 10%, were prepared to investigate how the abundant adsorption sites in this amine-rich polymer could enhance Cr (VI) removal. The adsorbent was a fluffy brown sponge. A schematic representation of the synthesis process has been provided in supporting information (**Figure S1**). **Figure S2 & 3** shows ATR-FTIR spectra and SEM image of the adsorbent, respectively. The ATR-FTIR spectrum of CS-PEI-GLA shows a combination of peaks from the two starting materials. The peak located at 3347 cm⁻¹ is the combination of stretching vibrations of –N–H and –O–H of the CS and PEI, and is slightly shifted, which indicates a stronger intramolecular hydrogen bonding (48). The peak located at 2961cm⁻¹ is attributed to PEI and corresponds to –C–H stretching. The peak located at 1616 cm⁻¹ is a result from the overlap of peaks from –N–H bending from both CS and PEI. These peaks confirm the

successful CS-PEI-GLA synthesis.

The XPS analysis of the adsorbents (**Table S2**) showed that by increasing the concentration of PEI in the reaction, the concentration of nitrogen increased and oxygen decreased in the final products, which supported the fact that higher amounts of PEI were incorporated into the adsorbents. The percent removal for the adsorbent with the highest PEI content, 10%, was expectedly higher than the others (**Figure S4**), where removal increased from 25 ± 2 % for 0% PEI to 93 ± 0 % for 10% PEI. Although some adsorption sites on CS were lost due to crosslinking with PEI (18), overall CS-PEI-GLA composites performed better than CS-GLA alone for Cr (VI) adsorption. The $\sim 70\%$ increase in chromium removal by adding PEI suggested that most of the adsorption sites were amine groups, while hydroxyl groups from CS contributed little for the adsorption. An attempt to synthesize a polymer composite with PEI content higher than 10% failed because a homogenous mixture of CS and PEI could not be achieved due to PEI viscosity. As a result, CS-PEI 10%-GLA was found to be the optimum adsorbent and was used for further experimentation. For the rest of the study, the optimized adsorbent will be referred to as CS-PEI-GLA.

3.1.2. Optimization of pH

An important factor playing a key role in the performance of the adsorbent for chromium removal is pH since it can change the properties of the functional groups present in the adsorbent as well as the stability of the adsorbent (49). Moreover, pH affects chromium oxidation states *i.e.* Cr (III) and Cr (VI) and their speciation (18, 31, 50, 51). Therefore, different parameters should be considered during pH optimization to explain its effect. The results (**Figure 1**) showed same removal (~ 90%) at pH values between 2 and 8, at higher pH values the removal decreased. The integrity of the adsorbent was not compromised in this pH range.

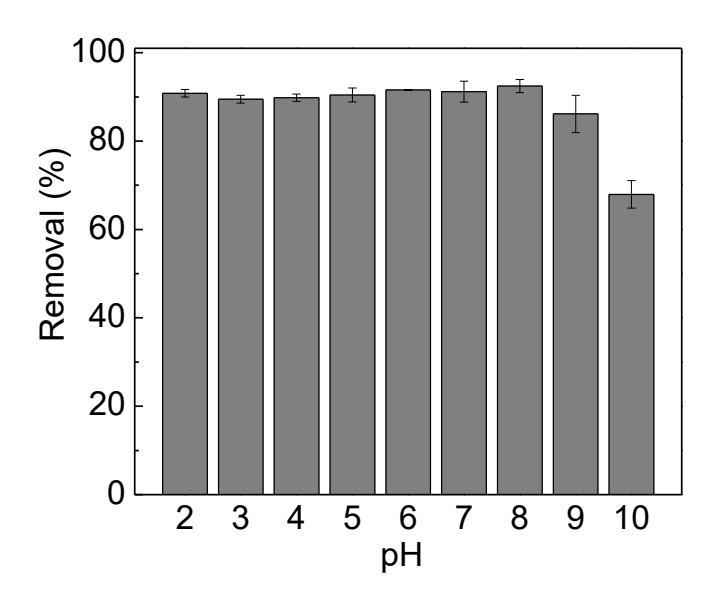


Figure 1: Effect of pH on chromium (100 mg/L) removal from a 20 mL solution by CS-PEI-GLA (20 mg) after 16 h. The standard deviation based on triplicate experiments are represented by the error bars.

As shown in our previous study (47) and **Figure S5**, the surface of the adsorbent is positively charged at the pH range 2-10 due to the protonation of amine and hydroxyl groups. However, a drastic decrease in surface charge was detected from pH 9 to 10. According to Cr (VI) speciation diagram (52) for the conditions tested in this study, at pH values between 2-5.5, Cr (VI) will be present in the solution as ~ 90% HCrO₄⁻ and 10% Cr₂O₇²-, then the concentration of both species will decrease, while CrO₄²- will increase with increasing pH. At pH 9, CrO₄²- is the only form of Cr (VI) existing in the solution. Since all the Cr (VI) ions are negatively charged, they can be attached to the positively charged surface of the adsorbent via electrostatic interaction (19, 31, 50, 53). Moreover, hydrogen bonds can form between amine groups and Cr (VI) species (49, 53). As pH increases, OH⁻ anions compete with Cr (VI) anions for adsorption sites (35), hence, removal decreases slightly at pH 9 compared to pH 8. This decrease is not significant, possibly because the conversion of HCrO₄⁻ to CrO₄²- leads to stronger electrostatic attraction between Cr (VI) anions

and the surface of the adsorbent, therefore, partially neutralizing the effects of increasing OH-concentrations. However, from pH 9 to 10, the removal dropped significantly, because of the increase in OH-concentration as well as decrease in surface charge of the adsorbent due to deprotonation of the amine groups.

Besides the anions, chromium in the cationic state, Cr (III), should be accounted for the removal. Cr (VI) can be reduced to Cr (III) in the presence of electron donors functional groups like hydroxyl and amine (15, 18, 49, 53, 54). After the reduction, amine groups on CS-PEI-GLA can chelate the cations (15, 49, 50, 55). Another possible mechanism for Cr (III) removal is its precipitation as Cr(OH)₃, especially at pH above 6 (49). To better understand the adsorption of chromium on the adsorbent, other parameters were investigated.

3.1.3. *Optimization of adsorbent dosage and contact time (kinetics)*

The dosage of the adsorbent determines how many adsorption sites would be available for the adsorbate; therefore, it can affect the percentage removal. As shown in **Figure S6**, CS-PEI-GLA can remove Cr (VI) completely from the solution at 0.5 g/L dosage. Therefore, this dosage was used for further experiments.

The rate of the adsorption and the right kinetic model describing the adsorption process are important for an efficient adsorption system design and to reveal the governing mechanisms in the adsorption process (56). **Figure 2** shows the adsorption capacity of CS-PEI-GLA over time from Cr (VI) solutions with 50, 100, and 250 mg/L concentration at pH=7. As can be seen in the figure, for 0.5 g/L dosage of the adsorbent at all three conditions, adsorption reaches equilibrium after 45 min. Therefore, an adsorption system with 45 min residence time can provide the maximum Cr (VI) removal from the aqueous phase by the adsorbent.

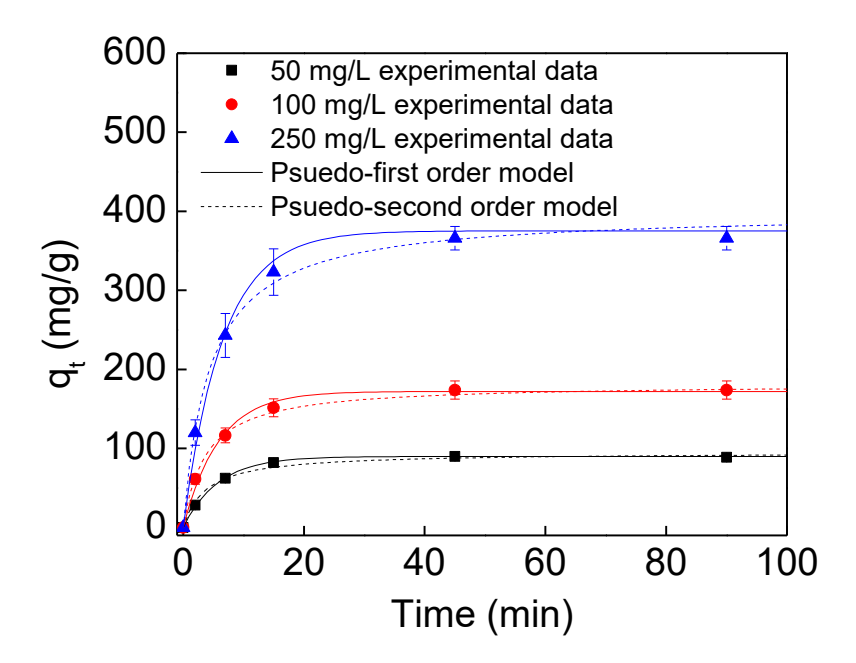


Figure 2: Experimental data and kinetic models for adsorption capacity over time (q_t) of CS-PEI-GLA (25 mg) in 50 mL solution at pH=7 with 50, 100, and 250 mg/L Cr (VI). The standard deviation based on triplicate experiments are represented by error bars.

These data were further studied by fitting them to the nonlinear form (57, 58) of the kinetic models: pseudo-first order and pseudo-second order. The rate constants (k₁ and k₂) and the calculated adsorption capacity (q_{e, cal}) were obtained by fitting. As presented in **Table 1**, the goodness-of-fit value for both models were above 0.98 and q_{e, cal} was within the 7% range of the q_{eq, exp} in all the three conditions. However, as initial concentration of Cr (VI) increased, the R² for the pseudo-first order model decreased from 0.9983 to 0.9855 and the R² for the pseudo-second order model increased from 0.9878 to 0.9956. Same trend was observed for the difference between q_{eq, exp} and q_{e, cal}, as for the pseudo-first order model the difference between the two adsorption capacities increased from 2% to 7% with increase in initial concentration while the difference decreased from 4% to 1% for the pseudo-second order model.

Table 1: Adsorption kinetic parameters of Cr (VI) onto CS-PEI-GLA. The experiment was done with 25 mg of the adsorbent and 50 mL solution at pH=7, containing 50, 100, and 250 mg/L Cr (VI). $q_{eq, exp}$ (mg/g) is the batch experimental adsorption capacity at equilibrium, k_1 (1/min) is the rate constant for pseudo-first order model, $q_{e, cal}$ (mg/g) is the calculated adsorption capacity at equilibrium, R^2 is the goodness-of-fit value, and R^2 (g/mg.min) is the rate constant for pseudo-second order model.

| | | pseudo-first order | | | pseudo-second order | | | |
|-----------------------|----------------|--------------------|---------|----------------|---------------------|--------------------|----------------|--|
| Cr (VI) concentration | $q_{eq,\;exp}$ | k_1 | qe, cal | \mathbb{R}^2 | \mathbf{k}_2 | $q_{e,\text{cal}}$ | \mathbb{R}^2 | |
| (mg/L) | (mg/g) | (1/min) | (mg/g) | | (g/mg.min) | (mg/g) | | |
| 50 | 91.75 | 0.1730 | 89.85 | 0.9983 | 0.0028 | 95.09 | 0.9878 | |
| 100 | 174.70 | 0.1707 | 172.15 | 0.9908 | 0.0015 | 181.80 | 0.9947 | |
| 250 | 403.38 | 0.1530 | 375.34 | 0.9855 | 0.0006 | 399.52 | 0.9956 | |

Based on the features of the two kinetic models, it can be suggested that both diffusion and chemical adsorption is controlling the adsorption process, while the rate-limiting step at low concentrations is diffusion, and at high concentrations is the chemical adsorption that includes strong interactions between adsorption sites on the adsorbent and metal ions (59-61). In our previous study (47) we showed that the adsorbent has a porous structure with specific surface area of 462 m²/g, therefore the diffusion in the pores can be the rate-limiting step at low concentrations. At high concentrations, chemisorption, which was suggested as one of the involved mechanisms in section 3.1.2, controls the kinetic of the adsorption. Abundant amine functional groups on the adsorbent can form complexes with cations Cr (III), which were reduced from Cr (VI), due to the presence of electron donor functional groups like hydroxyl and amine (15, 49, 50). It should also be noted that the k₂ value decreased from 0.0028 to 0.0006 (g/mg.min) when initial concentration

increased, which shows that the adsorption process highly depends on the concentration (62). To further identify characteristics of the adsorption process, the effect of Cr (VI) concentration and adsorption isotherms were investigated.

3.1.4. Effect of Cr (VI) initial concentration and isotherms

The concentration of the adsorbate can affect the adsorption process. Moreover, data obtained from the adsorption at various initial concentrations can be used to determine the parameters in adsorption isotherms. These mathematical models can provide valuable information about the characteristics of the adsorbent that can be used in the design of an adsorption system, namely: maximum adsorption capacity, adsorption sites, and their homogeneity (59, 63, 64). The equilibrium concentration and adsorption capacity data, after adsorption started at 20, 50, 100, 250, and 500 mg/L, were used to determine the model parameters of 2 two-parameter models: Langmuir and Freundlich and 3 three-parameter models: Redlich-Peterson, Sips, and Toth. For the two-parameter models, the adsorption system was better described with the Langmuir model rather than Freundlich (Figure 3 (a) and Table 2) and for the three-parameter models, Sips had the best fitting (Figure 3 (b) and Table 2). However, the R² for all the three-parameter models was > 0.97, since these models inherently have less error in fitting to the experimental data because of the higher number of parameters (65).

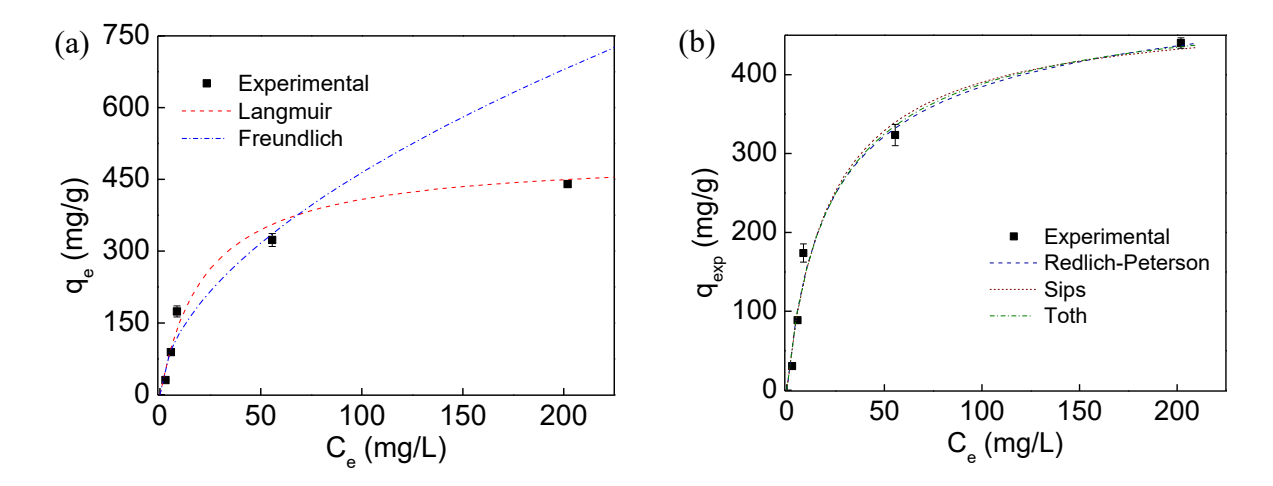


Figure 3: Experimental data at equilibrium with (a) two-parameter isotherm models and (b) three-parameter isotherm models. The q_{eq} (mg/g) is the adsorption capacity at equilibrium and C_e (mg/L) is the Cr (VI) concentration in the solution at equilibrium. Adsorption was done for five Cr (VI) solution with 20, 50, 100, 250, and 500 mg/L concentration by adding 0.5 g/L of the adsorbent for 2 h. The standard deviation based on triplicate experiments are represented by the error bars.

Table 2: Isotherm models' parameters and goodness-of-fit (R²) of Cr (VI) adsorption onto CS-PEI-GLA obtained by nonlinear method. Adsorption was done for five Cr (VI) solution with 20, 50, 100, 250, and 500 mg/L concentration by adding 0.5 g/L of the adsorbent for 2 h.

| Langmuir | Freundlich | Redlich-Peterson | Sips | Toth |
|------------------------|-----------------|--------------------|------------------|------------------|
| $R^2 = 0.9862$ | $R^2 = 0.8370$ | $R^2 = 0.9793$ | $R^2 = 0.9922$ | $R^2 = 0.9782$ |
| $q_{\text{max}} = 500$ | $K_F = 30.2018$ | $A_{RP} = 25.7585$ | $q_s = 488.4890$ | $q_t = 512.8120$ |
| $K_L = 0.0344$ | 1/n = 0.5547 | $B_{RP} = 0.0808$ | $K_s = 0.0430$ | $K_t = 0.0515$ |
| | | g=0.9239 | $n_s = 1.0566$ | t=0.8253 |

The fact that Langmuir model described the system well was confirmed not only by the goodness-of-fit value but also by n_s from the Sips model, since it was close to one (64). The Langmuir model assumes the adsorbent's surface to be homogenous and the adsorption to be a monolayer (59, 60, 66). The adsorption being monolayer was further confirmed as the parameter g from Redlich-Peterson and t from the Toth models were close to unity (67, 68). As discussed in section 3.1.2, hydroxyl and amine groups are the adsorption sites on CS-PEI-GLA, however, the abundance of amine groups in the adsorbent makes them the dominant adsorption sites (18). The adsorption capacity from Sips model (488.49 mg/g) was close to maximum adsorption capacity obtained from the Langmuir model (500 mg/g). When compared to q_{max} of similar adsorbents in the literature, it was found that the Langmuir q_{max} for CS-PEI-GLA was significantly higher (**Table S3**).

3.1.5. The effect of temperature and thermodynamics

Along with the isotherms, thermodynamic concepts can further elaborate the adsorbent behavior. **Figure S7** shows the Cr (VI) adsorption capacity onto CS-PEI-GLA at different temperatures, and it was observed the Q_e increased with the rise in temperature. The thermodynamic parameters Gibb's free energy (ΔG°), the enthalpy (ΔH°), and the entropy (ΔS°) change were calculated from the **Equations S11 to S13**. The determined values are shown in **Table S4**. The negative values of ΔG° at different temperatures confirmed that adsorption process is spontaneous and feasible. The enthalpy change was 18.10 kJ/mol, which indicated the endothermic nature of the adsorption process. The positive value of entropy change suggests an increase in the randomness at the solid-solution interface during the adsorption process (69-71).

3.1.6. Effect of coexisting ions

The presence of other ions in water can influence the chromium removal, because electrostatic interactions play an important role in the adsorption process (72, 73). Experiments were performed to evaluate the effect of Cl⁻, NO₃-SO₄²⁻, PO₄³⁻, Cd²⁺, and Zn²⁺ at different concentrations. As shown in **Figure 4**, the chromium removal capacity was affected by all ions, however, with different levels of influence.

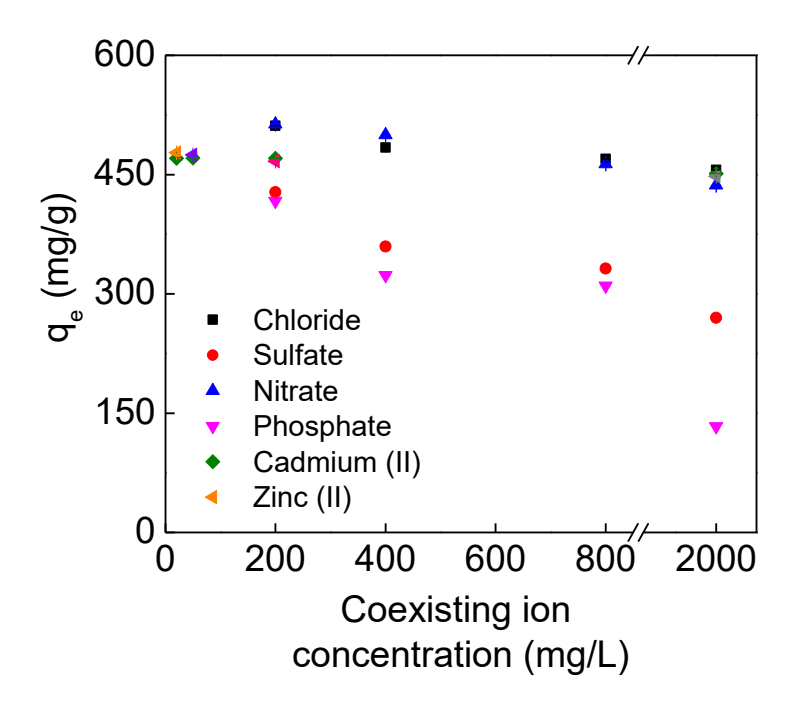


Figure 4: The effect of coexisting ions on the Cr (VI) adsorption. Experiments were performed at pH 7 with 100 ppm Cr (VI) solution and Cl⁻, NO₃⁻, SO₄²⁻, PO₄³⁻ in a range of concentration from 200 to 2000 mg/L. For Cd²⁺ and Zn²⁺ the concentration range were between 20 and 2000 mg/L. The standard deviation based on triplicate experiments are represented by error bars.

The Cl⁻ and NO₃⁻ had no remarkable effect on the adsorption process, even when the concentration of those anions increased. However, when the SO₄²⁻ and PO₄³⁻ concentration increased from 200 to 2000 ppm, the removal capacity decreased substantially. Moreover, it was noticed that the effect

of PO₄³⁻ was greater than SO₄²⁻. This could be attributed to charge that each anion possesses (70, 74). According to Cr (VI) speciation diagram, Cr (VI) is mostly present as CrO₄²⁻ at pH 7; therefore, monovalent ions of Cl⁻ and NO₃⁻ could slightly compete with Cr (VI) for positive charges on the CS-PEI-GLA surface. On the other hand, the SO₄²⁻ and PO₄³⁻ are bivalent and trivalent anions, respectively, and they may greatly compete with Cr (VI) for more sites on the adsorbent. These results were consistent with the previous investigations (72-75). For Cd and Zn, the presence of ions in the concentration range between 20 and 200 ppm, slightly decreased the chromium removal capacity. However, when the cation concentration increased to 2000 ppm, it was observed a significant decrease in the removal capacity. This can be explained by the fact that those cations might combine with chromium anions, which leads to a reduction of the adsorption efficiency (76). Nonetheless, the presence of anions seems to play a major role in chromium adsorption.

3.2. Optimization of Cr (VI) removal: Column process

3.2.1. Optimization of flow rate for Cr (VI) removal

One of the most important factors for real adsorption applications that cannot be assessed by batch studies, is flow rate. According to **Figure S9 (a) and Table 3**, the breakthrough curves shifted to the left when the flow rate increased from 5 mL/min to 7.5 mL/min and 10 mL/min, resulting in smaller breakthrough time, volume of clean water, and adsorption capacity. When the flow rate increased, a higher load of chromium ions entered the column with a shorter residence time, therefore, the column met the breakthrough point quicker (77). An increase in flow rate can increase adsorption capacity by reducing the mass transfer resistance, (77, 78) or decrease adsorption capacity by decreasing the residence time (79). The short residence time interferes with

the equilibrium between the ions and adsorbent, as a result, the adsorbent cannot reach its full adsorption capacity (77, 79). As shown in **Table 3**, for the conditions tested in this study, the effect of residence time was dominant and the lowest flow rate yielded the highest adsorption capacity.

Table 3: The parameters of the continuous mode (column) experiments. Q (mL/min) is the rate of flow, C_0 (mg/L) is the concentration of chromium in the influent, L (cm) is the height of the packed-bed, M (g) is the amount of the adsorbent, t_b (min) is breakthrough time, q_{exp} (mg/g) is experimental adsorption capacity, and V_b (mL) is the volume of clean water obtained before breakthrough point.

| Run# | Q (mL/min) | C ₀ (mg/L) | L (cm) | M (g) | t _b (min) | q _{exp} (mg/g) | V _b (mL) |
|------|------------|-----------------------|--------|-------|----------------------|-------------------------|---------------------|
| 1 | 5 | 225 | 7 | 0.5 | 150 | 594.76 | 750 |
| 2 | 7.5 | 225 | 7 | 0.5 | 73 | 376.18 | 549 |
| 3 | 10 | 225 | 7 | 0.5 | 42 | 324.36 | 425 |
| 4 | 5 | 100 | 7 | 0.5 | 200 | 370.02 | 1000 |
| 5 | 5 | 500 | 7 | 0.5 | 68 | 562.76 | 340 |
| 6 | 5 | 225 | 3.5 | 0.25 | 110 | 753.12 | 550 |
| 7 | 5 | 225 | 10.5 | 0.75 | 220 | 522.51 | 1100 |

Table S5 shows how the different parameters of the models change with change in the flow rate. The dual effects of flow rate can be observed in this table. While the constant rate of the models increased at higher flow rates, the q_{exp} changed in the opposite direction. The decrease in mass transfer resistance at higher flow rates resulted in higher rate constants. On the other hand, the adsorption capacity was lower because of the lower residence time (78). The comparison of the experimental adsorption capacity (q_{exp}) with the predicted adsorption capacity from the Thomas model (q_m), showed less than a 4% difference for all three conditions. Therefore, the models were able to accurately represent the characteristics of the column.

3.2.2. Effect of influent concentration on Cr (VI) removal

342

343

344

345

346

347

348

349

350

351

352

353

354

355

356

357

358

359

360

361

362

363

364

To evaluate how the adsorption system can be used to clean up contaminated water from different sources with different amounts of chromium ions, it is important to investigate how the concentration of chromium in the influent affects the adsorption operation. According to Figure **S9** (b) the breakthrough curves were moved to the left by an increase in the Cr (VI) concentration from 100 to 225 and 500 mg/L. Therefore, as presented in **Table 3**, t_b was the shortest at 500 mg/L and the longest at 100 mg/L. Similarly, V_b was the lowest at 500 mg/L and the highest at 100 mg/L. This is because when the number of chromium ions increased in the flow, the saturation of the column happened faster (77). In terms of q_{exp}, however, the trend was not straightforward. It is expected that higher concentrations will lead to a higher concentration gradient between the adsorbent surface and the bulk of the solution, therefore, providing higher mass transfer force (77, 78). When the mass transfer force increases, the adsorbent becomes saturated faster, as a result adsorption capacity increases (77). This is true as q_{exp} , as well as q_m , were the lowest for 100 mg/L compared to the highest concentrations, however, these two adsorption capacities were almost similar when 225 and 500 mg/L were compared (**Table 3**). This might be because at 5 mL/min flow rate, the concentration gradient for 225 mg/L was high enough for the adsorbent to reach equilibrium, therefore increasing the influent concentration to 500 mg/L did not further increase the adsorption capacity. High goodness-of-fit and less than 5% difference between $q_{\text{\rm exp}}$ and $q_{\text{\rm m}}$ (**Table 3 & S5**) showed that the models described the adsorption system well.

3.2.3. Optimization of bed height for Cr (VI) removal

The role of bed height on the adsorption properties of a column needs to be determined for a real application design. The main effect of the bed height is on the abundance of adsorption sites and the flow residence time in the packed-bed (80). Furthermore, bed height may affect the physical

properties of the packed bed like compaction of the bed and how the flow passes through the bed (79). Figure S9 (c) and Table S5 showed that longer breakthrough time and larger V_b were obtained at higher bed height. These results are the effect of the increase in adsorption sites for the chromium ions due to increase in bed height. Therefore, it took longer for the column to reach the breakthrough point. It is expected that with longer contact time, the system comes closer to the equilibrium and the adsorption capacity increases (77). However, in this study, the smallest bed height showed the highest q_{exp} (and q_m), which is probably due to compaction of the adsorbent, channeling of the flow, and the unused adsorbent on the side of the column at high bed heights (79). These effects on the adsorption system exacerbated for 10.5 cm bed, as the goodness-of-fit was the lowest (Table S5) compared to the other conditions throughout the whole study. The models did not predict the breakthrough curve accurately, although q_m and q_{exp} were in good agreement. Based on these results, a low bed height is recommended for this adsorbent for effective removal of Cr (VI).

3.3. Recovery of CS-PEI-GLA in batch and continuous modes and adsorption mechanism

For environmental (less sludge production) and economical (less operational costs) reasons, it is important to desorb the absorbate from the adsorbent and use it for multiple rounds of adsorption (81). Different recovery agents were used to desorb chromium ions from CS-PEI-GLA. According to **Figure S10 (a)**, NaOH 0.1 M presented the best desorption performance (67 \pm 3 %) compared to the other agents. A complete desorption of chromium ions from the adsorbent was achieved (data not shown) by HNO₃ 2M at the expense of dissolving the adsorbent. Therefore, NaOH was identified as the best recovery agent. However, this recovery agent could not completely regenerate the adsorbent. Additionally, NaOH at higher concentrations did not improve the recovery as shown in **Figure S11**. The same outcome was observed for regeneration of the column with NaOH 0.1 M

solution, where the recovery was even lower compared to the batch study, as about 31% of the chromium ions were recovered (Figure S10 (b)). However, it should be noted that recovery was fast and almost all the recoverable adsorbates were desorbed in the first 10 minutes. The fact that the adsorbent cannot be completely recovered was further revealed when multiple cycles of adsorption/desorption were done with NaOH 0.1 M. Since part of the chromium ions remained on the adsorption sites, after each cycle, the amount of chromium ions adsorbed to the adsorbent decreased in each cycle (Figure S10 (c)). Low recovery of chromium ions from amine-rich adsorbents have been reported in the literature before. Gonzalez Lopez et al. (77) used CS supported on a porous material to adsorb chromium. In regeneration of the adsorbent, a maximum of 62% recovery was achieved. About the same recovery percentage was reported by Zhang et al. (15) when they used a PEI/amyloid fibrils/polyvinyl alcohol aerogel beads as the adsorbent. Geng et al. (50) investigated the performance of a PEI-graphene oxide adsorbent for Cr (VI) removal, but they did not investigate the regeneration of the adsorbent. To understand the low recovery of chromium, XPS and FTIR spectra of CS-PEI-GLA and CS-PEI-GLA-Cr were studied. As illustrated in **Figure S12** the XPS total survey spectra, the binding energies at 285, 400, and 533 eV were related to C 1s, N 1s, and O 1s, respectively. For the spectrum of CS-PEI-GLA-Cr, two peaks at 576 and 585 eV appeared, which were related to Cr 2p3/2 and Cr 2p1/2 orbits, respectively, demonstrating that Cr (VI) was successfully adsorbed by CS-PEI-GLA (72, 73, 75). The FTIR spectra (Figure S13) of the adsorbent after adsorption with Cr showed two new sharp peaks at 783 and 902 cm⁻¹ belonging to chromium ions compared to the adsorbent before adsorption (54, 82). The intensity of the broad peak in the 2600-3600 cm⁻¹ range due to stretching vibration of -N-H and -O-H groups decreased, which shows the interaction of

388

389

390

391

392

393

394

395

396

397

398

399

400

401

402

403

404

405

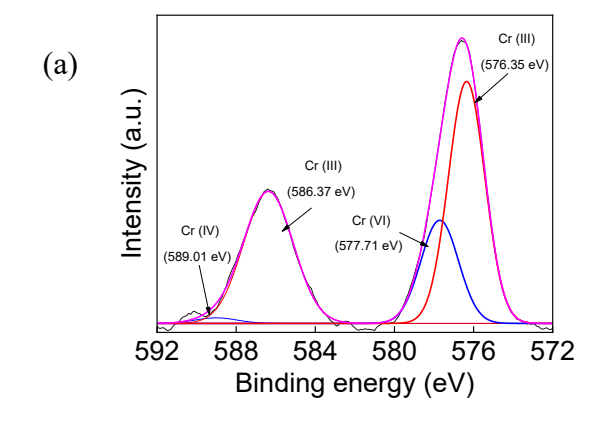
406

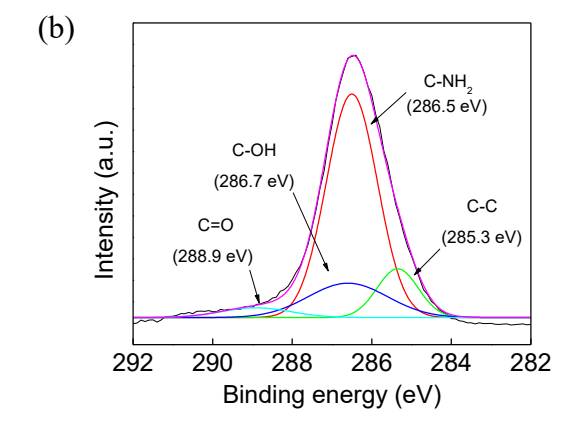
407

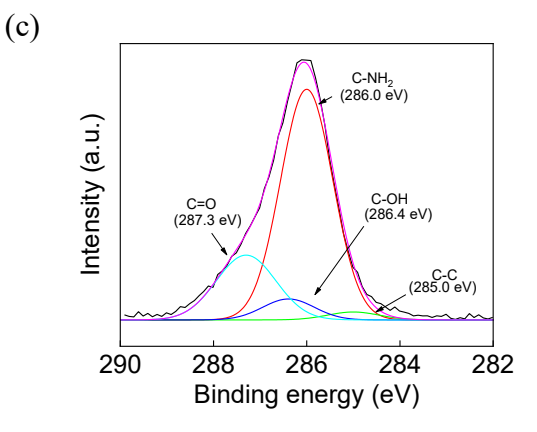
408

409

amine and hydroxyl groups with chromium ions (82). The involvement of amine groups in the adsorption was further confirmed by the shifting of -N-H bending at 1608 cm⁻¹ in the pristine adsorbent to 1653 cm⁻¹ in the saturated adsorbent (82). High-resolution XPS spectra of Cr2p for CS-PEI-GLA-Cr showed four peaks at 576 and 586, which were assigned to Cr (III), and at 577 and 589, which were assigned to Cr (VI) (18) (**Figure 5 (a)**). In CS-PEI-GLA-Cr, the Cr (III) peak presented a higher intensity than the Cr (VI) peak, which confirmed chromium reduction (15, 38, 72).







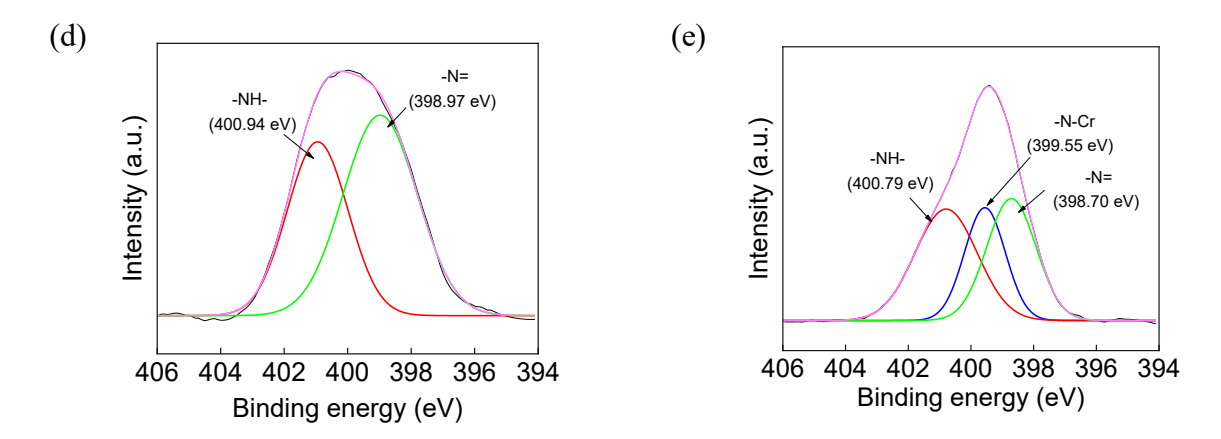


Figure 5: (a) XPS spectra of Cr 2p3/2 for CS-PEI-GLA after exposure to Cr (VI) solution. XPS C 1s high-resolution spectra of (b) CS-PEI-GLA and (c) CS-PEI-GLA-Cr. XPS N 1s high-resolution spectra of (d) CS-PEI-GLA and (e) CS-PEI-GLA-Cr. Experiments were performed at pH 7 with 100 ppm Cr (VI).

As discussed in Section 3.1.2. at the condition in our study, $Cr_2O_7^{2-}$ converts to $HCrO_4^-$. The $HCrO_4^-$ is a highly reducible species (+ 1.35 V). Therefore, in the presence of an electron donor, the reduction reaction might occur according to the following equation, resulting in the conversion of Cr (VI) to Cr (III) (18, 52, 75):

423
$$HCrO_4^- + 7H^+ + 3e^- \rightleftharpoons Cr^{3+} + 4H_2O$$
 Equation (8)

Figure 5 shows the high-resolution XPS spectra of C 1s (b&c) and N 1s (d&e) for the adsorbent before and after the chromium adsorption process. CS-PEI-GLA C 1s spectrum shows four peaks at 285.3 and 286.5, attributed to C-C bond and C-NH₂ from amines groups from both chitosan and PEI, and 286.7, and 288.9 attributed to C-OH, and C=O bonds from chitosan, respectively (4, 52, 83). CS-PEI-GLA N 1s spectrum presented peaks at 400.94 for -NH- and 398.87 for -N=. **Table 4** shows the contribution of each functional group. The peak at 286.5 eV, attributed to the C-NH₂

bond, was more pronounced than the other peaks (67.8%) due to the high concentration of PEI on the adsorbent.

Table 4: Percentage abundance of the functional group of CS-PEI-GLA and CS-PEI-GLA-Cr based on the area of the fitted XPS peaks.

| Sample | C-C/C=C | C-NH ₂ | С-ОН | C=O | -NH- | -N= | -N-Cr |
|---------------|---------|-------------------|------|------|------|------|-------|
| CS-PEI-GLA | 11.9 | 67.8 | 16.2 | 4.0 | 41.5 | 58.5 | 0 |
| CS-PEI-GLA-Cr | 2.3 | 69.4 | 6.2 | 22.1 | 39.5 | 34.2 | 26.3 |

Compared to unused CS-PEI-GLA, C 1s spectrum of used CS-PEI-GLA presented a more pronounced peak for C=O (22.1%) while the intensity of C-OH reduced from 16 to 6%, indicating the occurrence of oxidation reactions as suggested in the following equations (18, 38, 72, 75).

437
$$R-CH_2-OH+Cr(VI) \rightarrow R-(C=O) H+Cr(III) Equation (9)$$

438
$$R-(C=O) H+ Cr(VI) \rightarrow R-COOH + Cr(III)$$
 Equation (10)

For N 1s spectrum, after the chromium adsorption, both amino (400.94 eV) and imine (398.87 eV) peaks intensity decreased considerably and a new peak was observed at 399.55 eV, which was assigned to N-Cr, indicating that amino groups from CS-PEI-GLA participated in the Cr(VI) removal process (44, 84).

$$-NH_2 + H^+ \rightarrow -NH_3^+$$
 Equation (11)

444
$$-NH_3^+ + HCrO_4^- \rightarrow -NH_3^+ \dots HCrO_4^-$$
 Equation (12)

445
$$-N^{+}=CH_{2}+HCrO_{4}^{-} \rightarrow -N^{+}=CH_{2}.....HCrO_{4}^{-}$$
 Equation (13)

After the recovery with NaOH, the intensity of the peaks at 783 and 902 cm⁻¹ belonging to the chromium ions drastically decreased. This observation along with the increase in the intensity of

the broad band from 2600 to 3600 cm⁻¹ revealed that most of the chromium ions have been removed from the adsorption sites. However, the -N-H bending was still present at 1653 cm⁻¹ and the broad band from 2600 to 3600 cm⁻¹ was not as intense as the pristine adsorbent, showing that some of the amine groups were still attached to the chromium ions after recovery (54).

Based on the XPS and FTIR data, the desorption happened when the amine groups got deprotonated at basic pHs, therefore, chromium ions were released to the solution (19, 60). However, the low recovery of chromium ions could be attributed to the reduction of Cr (VI) to Cr (III) by hydroxyl and amine groups followed by chelation with the amine groups (38, 85). NaOH was able to recover the electrostatically attached Cr (VI) ions on the surface of the adsorbent by deprotonation of the functional groups, however, if the metal ions were chelated by the amine groups, they could not be removed by a change in pH (18, 77, 82). Figure 6 shows the adsorption mechanism.

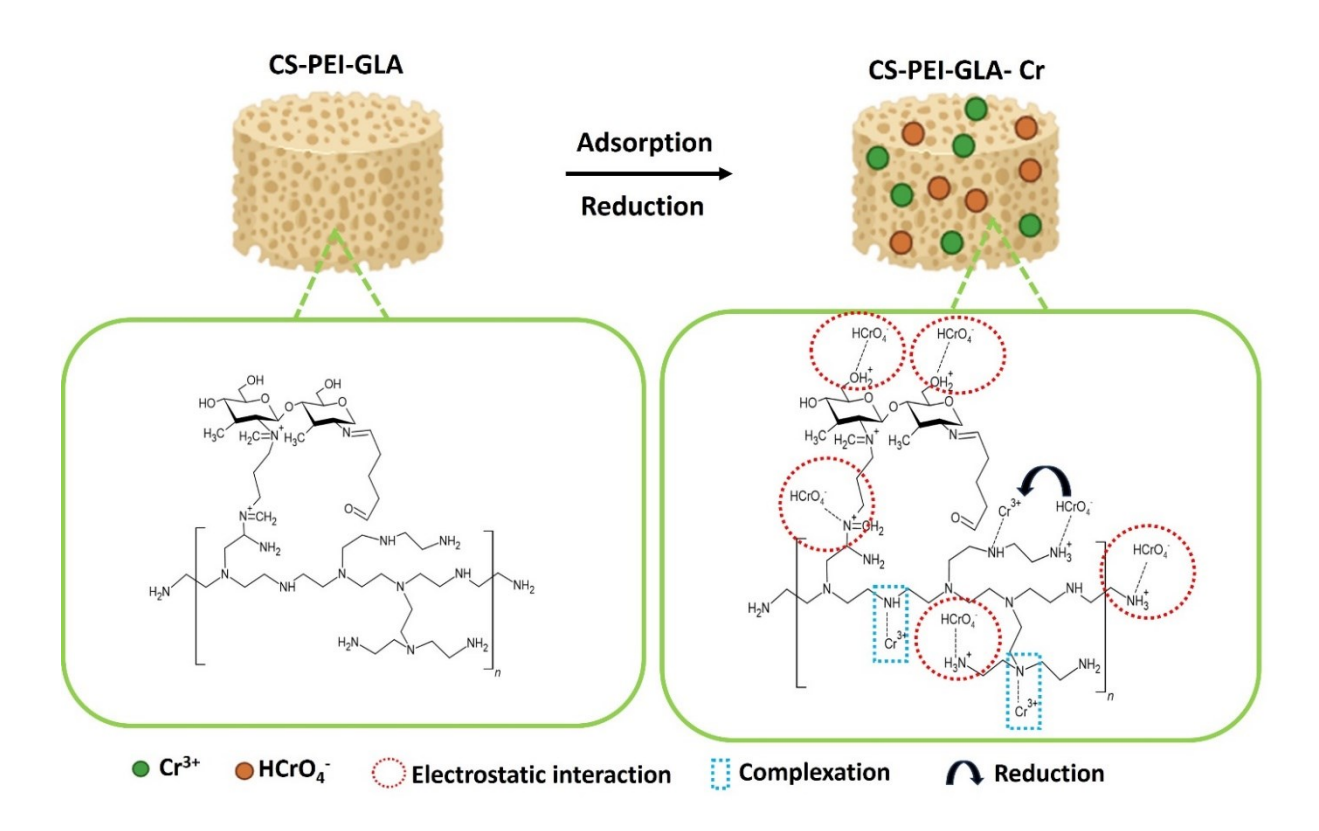


Figure 6: Schematic diagram of Cr (VI) adsorption mechanism on CS-PEI-GLA

Although CS-PEI-GLA could not be completely regenerated, it could be converted from Cr (VI) to a less toxic form of chromium, i.e. Cr (III) (18, 53). Moreover, the adsorbent could be incinerated to obtain less sludge for disposal.

3.4. Removal of chromium from electroplating wastewater in batch and continuous modes

Chromium electroplating wastewater is highly polluted with chromium ions; therefore, it is important to treat this wastewater before releasing it into the environment. The electroplating wastewater with 263 mg/L of chromium was treated with the adsorbent. Detailed characteristics of the wastewater is presented in **Table S6**. The batch study showed that CS-PEI-GLA can remove 97.1 ± 0.1 % of the chromium after 1 h. When the wastewater was passed through the column with 0.25 g of the adsorbent, less than 2 mg/L chromium was detected in the effluent after treating 750

mL of the wastewater, after that the chromium concentration drastically increased and the column became completely saturated with 1650 mL of the wastewater (**Figure 7**). These results demonstrate that CS-PEI-GLA is effective in chromium removal in both batch and continuous modes from the complicated chemistry of electroplating wastewater.

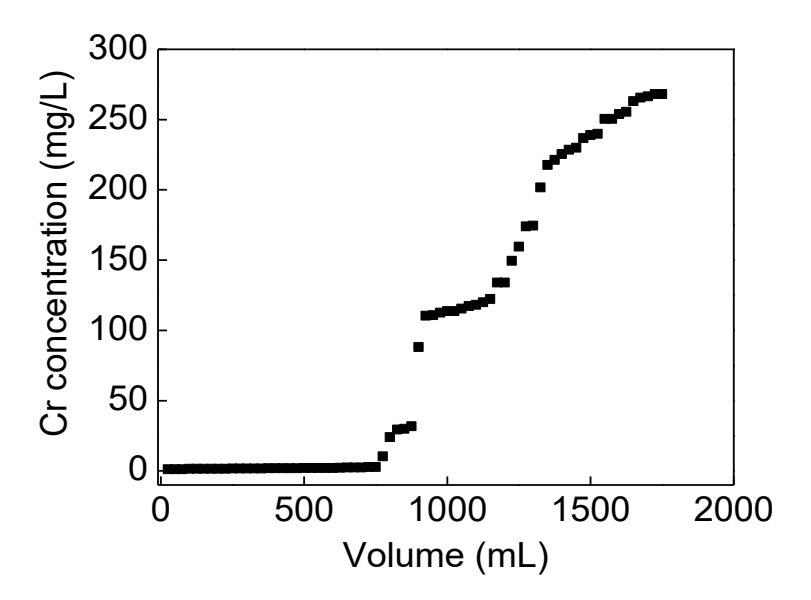


Figure 7: Breakthrough curve for chromium removal from electroplating wastewater. The flow rate was 5 mL/min and 0.25 g (3.5 cm) packed-bed of CS-PEI-GLA was used. The initial chromium concentration was 263 mg/L.

4. Conclusion

A polymer composite with some hydroxyl and abundant amine functional groups was prepared through a simple synthesis method by incorporating the soluble PEI into a support matrix of CS via crosslinking with GLA. The adsorbent with 10% PEI had the best chromium removal compared to 0, 2, and 5%, highlighting the crucial role of amine groups for Cr (VI) adsorption. The importance of amine groups was further confirmed when more than 90% chromium removal was

achieved over a wide range of pH values (2-8) but decreased at pH 9-10 due to deprotonation of the amine groups. The pseudo-first order was the governing kinetic model at low concentrations, while at high concentrations the adsorption process was controlled by the pseudo-second order model. Langmuir isotherm showed the adsorption sites are homogenous and a maximum adsorption capacity of 500 mg/g. The adsorbent was mostly selective toward chromium ions as a reduction of adsorption capacity was only observed when di- and tri-valent anions existed at concentrations four times or more than Cr (VI). FTIR and XPS analysis showed reduction of Cr (VI) to Cr (III) on the surface by hydroxyl and amine groups, which explained the low recovery of the adsorbent with NaOH. Amine groups that electrostatically adsorbed Cr (VI) could release the chromium ion because of deprotonation as a result of the increased pH. However, chromiumloaded amine groups, could not be recovered, because the Cr (VI) on those amine groups were reduced to Cr (III) and the increase in pH could not affect the amine Cr (III) complex. The adsorbent was used in continuous mode to investigate practical applications. Adsorption capacity decreased by an increase in flow rate due to shorter residence time. An increase in influent concentration from 100 to 225 mg/L increased adsorption capacity, but from 225 to 500 mg/L same q_{exp} was obtained, most likely because the adsorbent reached equilibrium. An increase in the packed bed height decreased the q_{exp} due to changes in the characteristic of the flow, like channeling and compaction of the adsorbent. CS-PEI-GLA showed promise for practical removal of chromium by 97.1 ± 0.1 % of chromium from electroplating wastewater in batch mode and producing 750 mL of clean treated electroplating wastewater with a 3.5 cm packed bed.

483

484

485

486

487

488

489

490

491

492

493

494

495

496

497

498

499

500

501

| 503 | Funding |
|-----|---|
| 504 | This study was partially supported by the NSF BEINM and CHE (Grant Numbers: 170551 and |
| 505 | 1904472) fund, Welch Foundation award number (E-2011-20190330), and the NPRP12S-0307- |
| 506 | 190250. |
| 507 | Author contributions |
| 508 | Ali Ansari: Investigation, Formal analysis, Visualization, Writing-Original Draft. |
| 509 | Raynara Maria Silva Jacovone: Investigation, Formal analysis, Visualization, Writing-Original |
| 510 | Draft. |
| 511 | Enrico Tapire Nadres: Investigation, Formal analysis, Visualization. |
| 512 | Minh Đỗ: Investigation. |
| 513 | Debora F. Rodrigues: Conceptualization, Methodology, Validation, Supervision, Funding |
| 514 | acquisition, Writing-Review, and Editing. |
| 515 | |
| 516 | |
| 517 | |
| 518 | |
| 519 | |
| 520 | |
| 521 | |

References

- 523 1. Pakade VE, Tavengwa NT, Madikizela LM. Recent advances in hexavalent chromium removal
- from aqueous solutions by adsorptive methods. RSC Advances. 2019;9(45):26142-64.
- 525 2. Preethi J, Karthikeyan P, Vigneshwaran S, Meenakshi S. Facile synthesis of Zr4+ incorporated
- 526 chitosan/gelatin composite for the sequestration of Chromium(VI) and fluoride from water.
- 527 Chemosphere. 2021;262:128317.
- 528 3. Tangtubtim S, Saikrasun S. Adsorption behavior of polyethyleneimine-carbamate linked
- 529 pineapple leaf fiber for Cr(VI) removal. Applied Surface Science. 2019;467-468:596-607.
- 4. Liu B, Xin YN, Zou J, Khoso FM, Liu YP, Jiang XY, et al. Removal of Chromium Species by
- Adsorption: Fundamental Principles, Newly Developed Adsorbents and Future Perspectives. Molecules
- 532 (Basel, Switzerland). 2023;28(2).
- 533 5. Verma R, Maji PK, Sarkar S. Removal of hexavalent chromium from impaired water:
- Polyethylenimine-based sorbents A review. Journal of Environmental Chemical Engineering.
- 535 2023;11(2):109598.
- 6. Ramrakhiani L, Majumder R, Khowala S. Removal of hexavalent chromium by heat inactivated
- 537 fungal biomass of Termitomyces clypeatus: Surface characterization and mechanism of biosorption.
- 538 Chemical Engineering Journal. 2011;171(3):1060-8.
- 539 7. Ismael MNM, El Nemr A, El Ashry ESH, Abdel Hamid H. Removal of Hexavalent Chromium by
- 540 Cross-Linking Chitosan and N,N'-Methylene Bis-Acrylamide. Environmental Processes. 2020;7(3):911-30.
- 541 8. Krishna RH, Chandraprabha MN, Samrat K, Krishna Murthy TP, Manjunatha C, Kumar SG. Carbon
- nanotubes and graphene-based materials for adsorptive removal of metal ions A review on surface
- functionalization and related adsorption mechanism. Applied Surface Science Advances.
- 544 2023;16:100431.
- 545 9. Hu Z, Yang J, Liu M, Rao W, Xie Y, Yu C. Amine-functionalized cellulose nanofiber-sodium
- alginate-Fe(III) porous hollow beads for the efficient removal of Cr(VI). Cellulose. 2023;30(6):3807-22.
- 547 10. Gopal Reddi MR, Gomathi T, Saranya M, Sudha PN. Adsorption and kinetic studies on the
- removal of chromium and copper onto Chitosan-g-maliec anhydride-g-ethylene dimethacrylate.
- International journal of biological macromolecules. 2017;104:1578-85.
- 550 11. Sharma SK, Petrusevski B, Amy G. Chromium removal from water: a review. Journal of Water
- 551 Supply: Research and Technology-Aqua. 2008;57(8):541-53.
- 552 12. Islam MM, Mohana AA, Rahman MA, Rahman M, Naidu R, Rahman MM. A Comprehensive
- 553 Review of the Current Progress of Chromium Removal Methods from Aqueous Solution. Toxics
- 554 [Internet]. 2023; 11(3).
- 13. Irshad MA, Sattar S, Nawaz R, Al-Hussain SA, Rizwan M, Bukhari A, et al. Enhancing chromium
- removal and recovery from industrial wastewater using sustainable and efficient nanomaterial: A
- review. Ecotoxicology and Environmental Safety. 2023;263:115231.
- 558 14. Mitra S, Sarkar A, Sen S. Removal of chromium from industrial effluents using nanotechnology: a
- review. Nanotechnology for Environmental Engineering. 2017;2(1):11.
- 560 15. Zhang Y, Wen J, Zhou Y, Wang J, Cheng W. Novel efficient capture of hexavalent chromium by
- polyethyleneimine/amyloid fibrils/polyvinyl alcohol aerogel beads: Functional design, applicability, and
- mechanisms. Journal of Hazardous Materials. 2023;458:132017.
- 563 16. Wang H, Chen Y, Mo M, Dorsel P-KP, Wu C. Visualized adsorption and enhanced photocatalytic
- removal of Cr6+ by carbon dots-incorporated fluorescent nanocellulose aerogels. International journal
- of biological macromolecules. 2023;253:127206.
- 566 17. Zeng S, Long J, Sun J, Wang G, Zhou L. A review on peach gum polysaccharide: Hydrolysis,
- structure, properties and applications. Carbohydrate Polymers. 2022;279:119015.

- 568 18. Bandara PC, Peña-Bahamonde J, Rodrigues DF. Redox mechanisms of conversion of Cr(VI) to
- 569 Cr(III) by graphene oxide-polymer composite. Scientific Reports. 2020;10(1):9237.
- 570 19. Perez JVD, Nadres ET, Nguyen HN, Dalida MLP, Rodrigues DF. Response surface methodology as
- a powerful tool to optimize the synthesis of polymer-based graphene oxide nanocomposites for
- 572 simultaneous removal of cationic and anionic heavy metal contaminants. RSC Advances.
- 573 2017;7(30):18480-90.
- 574 20. Ansari A, Nadres ET, Đỗ M, Rodrigues DF. Investigation of the removal and recovery of nitrate by
- an amine-enriched composite under different fixed-bed column conditions. Process Safety and
- 576 Environmental Protection. 2021;150:365-72.
- 577 21. Vilela PB, Dalalibera A, Duminelli EC, Becegato VA, Paulino AT. Adsorption and removal of
- 578 chromium (VI) contained in aqueous solutions using a chitosan-based hydrogel. Environmental Science
- 579 and Pollution Research. 2019;26(28):28481-9.
- 580 22. Liu H, Yang F, Zheng Y, Kang J, Qu J, Chen JP. Improvement of metal adsorption onto
- 581 chitosan/Sargassum sp. composite sorbent by an innovative ion-imprint technology. Water Res.
- 582 2011;45(1):145-54.
- 583 23. Gokila S, Gomathi T, Sudha PN, Anil S. Removal of the heavy metal ion chromiuim(VI) using
- Chitosan and Alginate nanocomposites. International journal of biological macromolecules. 2017;104(Pt
- 585 B):1459-68.
- 586 24. Bhatt R, Sreedhar B, Padmaja P. Chitosan supramolecularly cross linked with trimesic acid -
- Facile synthesis, characterization and evaluation of adsorption potential for chromium(VI). International
- journal of biological macromolecules. 2017;104(Pt A):1254-66.
- 589 25. Sethy TR, Sahoo PK. Highly toxic Cr (VI) adsorption by (chitosan-g-PMMA)/silica
- 590 bionanocomposite prepared via emulsifier-free emulsion polymerisation. International journal of
- 591 biological macromolecules. 2019;122:1184-90.
- 592 26. Samuel MS, Bhattacharya J, Raj S, Santhanam N, Singh H, Pradeep Singh ND. Efficient removal of
- 593 Chromium(VI) from aqueous solution using chitosan grafted graphene oxide (CS-GO) nanocomposite.
- International journal of biological macromolecules. 2019;121:285-92.
- 595 27. de Castro Dantas TN, Dantas Neto AA, de A. Moura MCP, Barros Neto EL, de Paiva Telemaco E.
- 596 Chromium Adsorption by Chitosan Impregnated with Microemulsion. Langmuir. 2001;17(14):4256-60.
- 597 28. Huang R, Yang B, Liu Q. Removal of chromium(VI) lons from aqueous solutions with protonated
- 598 crosslinked chitosan. Journal of Applied Polymer Science. 2013;129(2):908-15.
- 599 29. Periyasamy S, Manivasakan P, Jeyaprabha C, Meenakshi S, Viswanathan N. Fabrication of nano-
- 600 graphene oxide assisted hydrotalcite/chitosan biocomposite: An efficient adsorbent for chromium
- 601 removal from water. International journal of biological macromolecules. 2019;132:1068-78.
- 602 30. Dima JB, Sequeiros C, Zaritzky NE. Hexavalent chromium removal in contaminated water using
- reticulated chitosan micro/nanoparticles from seafood processing wastes. Chemosphere. 2015;141:100-
- 604 11.
- 605 31. Vakili M, Deng S, Li T, Wang W, Wang W, Yu G. Novel crosslinked chitosan for enhanced
- adsorption of hexavalent chromium in acidic solution. Chemical Engineering Journal. 2018;347:782-90.
- 607 32. Kahu SS, Shekhawat A, Saravanan D, Jugade RM. Two fold modified chitosan for enhanced
- adsorption of hexavalent chromium from simulated wastewater and industrial effluents. Carbohydrate
- 609 Polymers. 2016;146:264-73.
- 610 33. Sessarego S, Rodrigues SCG, Xiao Y, Lu Q, Hill JM. Phosphonium-enhanced chitosan for Cr(VI)
- adsorption in wastewater treatment. Carbohydrate Polymers. 2019;211:249-56.
- 612 34. Shi T, Yang D, Yang H, Ye J, Cheng Q. Preparation of chitosan crosslinked modified silicon
- 613 material and its adsorption capability for chromium(VI). Applied Clay Science. 2017;142:100-8.
- 614 35. Hena S. Removal of chromium hexavalent ion from aqueous solutions using biopolymer chitosan
- coated with poly 3-methyl thiophene polymer. Journal of Hazardous Materials. 2010;181(1):474-9.

- 616 36. Hua C, Zhang R, Bai F, Lu P, Liang X. Removal of chromium (VI) from aqueous solutions using
- quaternized chitosan microspheres. Chinese Journal of Chemical Engineering. 2017;25(2):153-8.
- 618 37. Kekes T, Kolliopoulos G, Tzia C. Hexavalent chromium adsorption onto crosslinked chitosan and
- 619 chitosan/β-cyclodextrin beads: Novel materials for water decontamination. Journal of Environmental
- 620 Chemical Engineering. 2021;9(4):105581.
- 621 38. Wang Q, Zuo W, Tian Y, Kong L, Cai G, Zhang H, et al. An ultralight and flexible nanofibrillated
- 622 cellulose/chitosan aerogel for efficient chromium removal: Adsorption-reduction process and
- 623 mechanism. Chemosphere. 2023;329:138622.
- 624 39. Sarojini G, Kannan P, Rajamohan N, Rajasimman M. Bio-fabrication of porous magnetic
- 625 Chitosan/Fe3O4 nanocomposite using Azolla pinnata for removal of chromium Parametric effects,
- 626 surface characterization and kinetics. Environmental Research. 2023;218:114822.
- 627 40. Pillai CKS, Paul W, Sharma CP. Chitin and chitosan polymers: Chemistry, solubility and fiber
- formation. Progress in Polymer Science. 2009;34(7):641-78.
- 629 41. Wan Ngah WS, Teong LC, Hanafiah MAKM. Adsorption of dyes and heavy metal ions by chitosan
- composites: A review. Carbohydrate Polymers. 2011;83(4):1446-56.
- 42. Zhu W, Dang Q, Liu C, Yu D, Chang G, Pu X, et al. Cr(VI) and Pb(II) capture on pH-responsive
- 632 polyethyleneimine and chloroacetic acid functionalized chitosan microspheres. Carbohydrate Polymers.
- 633 2019;219:353-67.
- 634 43. Wang Q, Tian Y, Kong L, Zhang J, Zuo W, Li Y, et al. A novel 3D superelastic polyethyleneimine
- 635 functionalized chitosan aerogels for selective removal of Cr(VI) from aqueous solution: performance and
- mechanisms. Chemical Engineering Journal. 2021;425:131722.
- 637 44. Li R, An Q-D, Xiao Z-Y, Zhai B, Zhai S-R, Shi Z. Preparation of PEI/CS aerogel beads with a high
- density of reactive sites for efficient Cr(vi) sorption: batch and column studies. RSC Advances.
- 639 2017;7(64):40227-36.
- 640 45. Sun X, Yang L, Dong T, Liu Z, Liu H. Removal of Cr(VI) from aqueous solution using amino-
- 641 modified Fe3O4–SiO2–chitosan magnetic microspheres with high acid resistance and adsorption
- capacity. Journal of Applied Polymer Science. 2016;133(10).
- 643 46. Singh S, Arputharaj E, Dahms H-U, Patel AK, Huang Y-L. Chitosan-based nanocomposites for
- removal of Cr(VI) and synthetic food colorants from wastewater. Bioresource Technology.
- 645 2022;351:127018.
- 646 47. Nadres ET, Perez JVD, Rodrigues DF. High-capacity hydrogel polymer composite adsorbent for
- oitrate and phosphate removal from water. Proceedings of the Water Environment Federation.
- 648 2017(3):438-60.
- 649 48. Nie B, Stutzman J, Xie A. A Vibrational Spectral Maker for Probing the Hydrogen-Bonding Status
- of Protonated Asp and Glu Residues. Biophysical Journal. 2005;88(4):2833-47.
- 651 49. Deng S, Ting YP. Polyethylenimine-Modified Fungal Biomass as a High-Capacity Biosorbent for
- 652 Cr(VI) Anions: Sorption Capacity and Uptake Mechanisms. Environmental Science & Technology.
- 653 2005;39(21):8490-6.
- 654 50. Geng J, Yin Y, Liang Q, Zhu Z, Luo H. Polyethyleneimine cross-linked graphene oxide for removing
- 655 hazardous hexavalent chromium: Adsorption performance and mechanism. Chemical Engineering
- 656 Journal. 2019;361:1497-510.
- 657 51. Mishra S, Verma N. Carbon bead-supported hollow carbon nanofibers synthesized via
- 658 templating method for the removal of hexavalent chromium. Journal of Industrial and Engineering
- 659 Chemistry. 2016;36:346-54.
- 660 52. Gherasim C-V, Bourceanu G, Olariu R-I, Arsene C. A novel polymer inclusion membrane applied
- in chromium (VI) separation from aqueous solutions. Journal of Hazardous Materials. 2011;197:244-53.

- 662 53. Deng S, Long J, Dai X, Wang G, Zhou L. Simultaneous Detection and Adsorptive Removal of Cr(VI)
- lons by Fluorescent Sulfur Quantum Dots Embedded in Chitosan Hydrogels. ACS Applied Nano Materials.
- 664 2023;6(3):1817-27.
- 54. Das SK, Mukherjee M, Guha AK. Interaction of Chromium with Resistant Strain Aspergillus
- versicolor: Investigation with Atomic Force Microscopy and Other Physical Studies. Langmuir.
- 667 2008;24(16):8643-50.
- 668 55. Chen Z-L, Xu H, Bai L-Q, Feng Y-L, Li B. Protonated-amino-functionalized bamboo hydrochar for
- 669 efficient removal of hexavalent chromium and methyl orange. Progress in Natural Science: Materials
- 670 International. 2023;33(4):501-7.
- 671 56. Vahedi S, Tavakoli O, Khoobi M, Ansari A, Ali Faramarzi M. Application of novel magnetic β-
- 672 cyclodextrin-anhydride polymer nano-adsorbent in cationic dye removal from aqueous solution. Journal
- of the Taiwan Institute of Chemical Engineers. 2017;80:452-63.
- 674 57. Simonin J-P. On the comparison of pseudo-first order and pseudo-second order rate laws in the
- 675 modeling of adsorption kinetics. Chemical Engineering Journal. 2016;300:254-63.
- 58. Lima EC, Sher F, Guleria A, Saeb MR, Anastopoulos I, Tran HN, et al. Is one performing the
- 677 treatment data of adsorption kinetics correctly? Journal of Environmental Chemical Engineering.
- 678 2021;9(2):104813.
- 679 59. Ansari A, Vahedi S, Tavakoli O, Khoobi M, Faramarzi MAJAOC. Novel Fe3O4/hydroxyapatite/β-
- 680 cyclodextrin nanocomposite adsorbent: Synthesis and application in heavy metal removal from aqueous
- 681 solution. 2019;33(1):e4634.
- 682 60. Bandara PC, Perez JVD, Nadres ET, Nannapaneni RG, Krakowiak KJ, Rodrigues DF. Graphene
- Oxide Nanocomposite Hydrogel Beads for Removal of Selenium in Contaminated Water. ACS Applied
- 684 Polymer Materials. 2019;1(10):2668-79.
- 685 61. Wang J, Guo X. Adsorption kinetic models: Physical meanings, applications, and solving
- methods. Journal of Hazardous Materials. 2020;390:122156.
- 62. Hui M, Shengyan P, Yaqi H, Rongxin Z, Anatoly Z, Wei C. A highly efficient magnetic chitosan
- 688 "fluid" adsorbent with a high capacity and fast adsorption kinetics for dyeing wastewater purification.
- 689 Chemical Engineering Journal. 2018;345:556-65.
- 690 63. Ma J, Li J, Guo Q, Han H, Zhang S, Han R. Waste peanut shell modified with polyethyleneimine
- 691 for enhancement of hexavalent chromium removal from solution in batch and column modes.
- 692 Bioresource Technology Reports. 2020;12:100576.
- 693 64. Padmesh TVN, Vijayaraghavan K, Sekaran G, Velan M. Application of Two-and Three-Parameter
- 694 Isotherm Models: Biosorption of Acid Red 88 onto Azolla microphylla. Bioremediation Journal.
- 695 2006;10(1-2):37-44.
- 696 65. Sharifi S, Nabizadeh R, Akbarpour B, Azari A, Ghaffari HR, Nazmara S, et al. Modeling and
- optimizing parameters affecting hexavalent chromium adsorption from aqueous solutions using Ti-XAD7
- 698 nanocomposite: RSM-CCD approach, kinetic, and isotherm studies. J Environ Health Sci Eng.
- 699 2019;17(2):873-88.
- 700 66. Su M, Fang Y, Li B, Yin W, Gu J, Liang H, et al. Enhanced hexavalent chromium removal by
- 701 activated carbon modified with micro-sized goethite using a facile impregnation method. Science of The
- 702 Total Environment. 2019;647:47-56.
- 703 67. Yang J, Huang B, Lin M. Adsorption of Hexavalent Chromium from Aqueous Solution by a
- 704 Chitosan/Bentonite Composite: Isotherm, Kinetics, and Thermodynamics Studies. Journal of Chemical &
- 705 Engineering Data. 2020;65(5):2751-63.
- 706 68. Brdar M, Šćiban M, Takači A, Došenović T. Comparison of two and three parameters adsorption
- 707 isotherm for Cr(VI) onto Kraft lignin. Chemical Engineering Journal. 2012;183:108-11.
- 708 69. Aydın YA, Aksoy ND. Adsorption of chromium on chitosan: Optimization, kinetics and
- thermodynamics. Chemical Engineering Journal. 2009;151(1):188-94.

- 710 70. Hu X-j, Wang J-s, Liu Y-g, Li X, Zeng G-m, Bao Z-l, et al. Adsorption of chromium (VI) by
- 711 ethylenediamine-modified cross-linked magnetic chitosan resin: Isotherms, kinetics and
- 712 thermodynamics. Journal of Hazardous Materials. 2011;185(1):306-14.
- 71. Minh Thanh HT, Thu Phuong TT, Le Hang PT, Tam Toan TT, Tuyen TN, Mau TX, et al. Comparative
- 714 study of Pb(II) adsorption onto MIL-101 and Fe-MIL-101 from aqueous solutions. Journal of
- 715 Environmental Chemical Engineering. 2018;6(4):4093-102.
- 716 72. Zheng W, An Q, Lei Z, Xiao Z, Zhai S, Liu Q. Efficient batch and column removal of Cr(vi) by
- 717 carbon beads with developed nano-network. RSC Advances. 2016;6(106):104897-910.
- 718 73. Guo D-M, An Q-D, Xiao Z-Y, Zhai S-R, Shi Z. Polyethylenimine-functionalized cellulose aerogel
- 719 beads for efficient dynamic removal of chromium(vi) from aqueous solution. RSC Advances.
- 720 2017;7(85):54039-52.
- 721 74. Bahador F, Foroutan R, Esmaeili H, Ramavandi B. Enhancement of the chromium removal
- behavior of Moringa oleifera activated carbon by chitosan and iron oxide nanoparticles from water.
- 723 Carbohydrate Polymers. 2021;251:117085.
- 75. Li R, An Q-D, Mao B-Q, Xiao Z-Y, Zhai S-R, Shi Z. PDA-meditated green synthesis of amino-
- modified, multifunctional magnetic hollow composites for Cr(VI) efficient removal. Journal of the Taiwan
- 726 Institute of Chemical Engineers. 2017;80:596-606.
- 727 76. Dong L, Liang J, Li Y, Hunang S, Wei Y, Bai X, et al. Effect of coexisting ions on Cr(VI) adsorption
- onto surfactant modified Auricularia auricula spent substrate in aqueous solution. Ecotoxicology and
- 729 Environmental Safety. 2018;166:390-400.
- 730 77. González-López ME, Pérez-Fonseca AA, Arellano M, Gómez C, Robledo-Ortíz JR. Fixed-bed
- 731 adsorption of Cr(VI) onto chitosan supported on highly porous composites. Environmental Technology &
- 732 Innovation. 2020;19:100824.
- 733 78. Han X, Zhang Y, Zheng C, Yu X, Li S, Wei W. Enhanced Cr(VI) removal from water using a green
- 734 synthesized nanocrystalline chlorapatite: Physicochemical interpretations and fixed-bed column
- mathematical model study. Chemosphere. 2021;264:128421.
- 736 79. de Franco MAE, de Carvalho CB, Bonetto MM, de Pelegrini Soares R, Féris LA. Diclofenac
- removal from water by adsorption using activated carbon in batch mode and fixed-bed column:
- 738 Isotherms, thermodynamic study and breakthrough curves modeling. Journal of Cleaner Production.
- 739 2018;181:145-54.
- 740 80. Suksabye P, Thiravetyan P, Nakbanpote W. Column study of chromium(VI) adsorption from
- 741 electroplating industry by coconut coir pith. Journal of Hazardous Materials. 2008;160(1):56-62.
- 742 81. Ajmani A, Patra C, Subbiah S, Narayanasamy S. Packed bed column studies of hexavalent
- 743 chromium adsorption by zinc chloride activated carbon synthesized from Phanera vahlii fruit biomass.
- Journal of Environmental Chemical Engineering. 2020;8(4):103825.
- 745 82. Sun X-F, Ma Y, Liu X-W, Wang S-G, Gao B-Y, Li X-M. Sorption and detoxification of chromium(VI)
- 5746 by aerobic granules functionalized with polyethylenimine. Water Research. 2010;44(8):2517-24.
- 747 83. Jiang X, Liu Y, Yin X, Deng Z, Zhang S, Ma C, et al. Efficient removal of chromium by a novel
- biochar-microalga complex: Mechanism and performance. Environmental Technology & Innovation.
- 749 2023;31:103156.
- 750 84. Zong P, Cao D, Cheng Y, Wang S, Zhang J, Guo Z, et al. Carboxymethyl cellulose supported
- 751 magnetic graphene oxide composites by plasma induced technique and their highly efficient removal of
- 752 uranium ions. Cellulose. 2019;26(6):4039-60.
- 753 85. Sun Q, Zhang L, Wang C, Liu X, Lou C, Yang Y. High nitrogen content bimolecular co-
- 754 functionalized graphene nanoflakes for hypertoxic Cr(VI) removal: Insights into adsorption behavior and
- 755 mechanisms. Chemosphere. 2023;340:139804.